

Supplemental materials for “Impacts of transported background pollutants on summertime Western US air quality: model evaluation, sensitivity analysis and data assimilation”, by Huang et al. (2012)

This file includes text (Sections S1-S3), two tables and six figures.

S1. Clarification of absolute sensitivity calculations for MDA8 and W126

The absolute sensitivity calculations (e.g., Figures 4 and 5a-c) for MDA8 and W126 in this paper consistently followed the method below. Assuming we have O₃ time series from model simulations 1 and 2,

- a) Calculate MDA8 or W126 based on O₃ from simulation 1, Metric_SIM1
- b) Calculate MDA8 or W126 based on O₃ from simulation 2, Metric_SIM2
- c) Calculate MDA8 or W126 sensitivity: Metric_SIM1 – Metric_SIM2

where “Metric” stands for MDA8 or W126.

Especially for W126, this method is more practical than an alternative method that applies the weighting function to the sensitivity of O₃ time series themselves, because Metric_SIM1 and Metric_SIM2 are based on the simulation cases that represent possible scenarios.

S2. Impact of extrapolation methods on estimated TBG contribution to surface O₃ metrics

The estimated total TBG contributions to surface MDA8 or W126 (Fig. 4d) were calculated by equation S1:

extrapolated TBG contribution = extrapolated contribution from BC precursors + extrapolated contribution from BC O₃ (S1)

Fig. 3e-f demonstrated that surface W126 sensitivity to BC O₃ perturbations (second term on the right hand side of equation S1) had the strongest non-linearity. Here we compared the estimated TBG contributions to W126 when four different extrapolation methods were applied to calculate the extrapolated contribution from BC O₃. These extrapolation methods are described below:

For each grid cell, define **X** vector as the perturbations of 0.25, 0.5, 0.75 and 1 (base case), and **Y** vector as the surface W126 sensitivity to the corresponding perturbations in BC O₃, then:

Fit 1: $Y=aX^2+bX+c$

Fit 2: $Y=aX^2+c$

Fit 3: As the Fig. S1e black thick line shows, the three slopes (for X in [0.25,0.5], [0.5,0.75], and [0.75,1.0]) decreased by ~half. Based on this trend, we extrapolated from the sensitivity to 75% reduction in BC O₃, using the slope that is ½ of the previous line (X in [0.25,0.5]).

Fit 4: $Y=bX+c$

Fig. S1a-d show the resulting extrapolated results at surface based on these four fitting methods. Fig. S2 compare the absolute and relative differences. Fig. S1e is the demonstration of the calculations for the second term on the right hand side of equation S1 when using the mean sensitivities over Regions 9 and 10 (refer to Fig. 3f). The different methods can result in >40% of differences in the extrapolated TBG contributions over certain regions. In the main text (Sections 3.1.3 and 3.1.4 and Fig. 4d) we used results based on Fit 1, because of the smallest residuals and highest r-square values.

For W126, the first term on the right hand side of equation S1 was calculated by linearly extrapolated from 75 % reduction in the BC precursors (i.e., 4/3 of this sensitivity). For MDA8, both terms on the right hand side of equation S1 were also calculated by using this linear extrapolation method.

S3. Exploration of the biases in TBG contributions

We explored the relationships between the biases in the base simulation and the estimated TBG contributions. Lin et al. (2012b) correlated model biases with stratospheric contributions estimated by the AM3 model on a ~50 km horizontal resolution in Spring 2010. The r^2 value was ~0.4 when observed MDA8 exceeded 60 ppb and decreased to ~0.2-0.3 for all points with positive biases. They concluded that the correlations did not necessarily indicate a systematic model overestimate of stratospheric contribution to high-O₃ events. We quantitatively explored the relationship between model biases and the estimated TBG contributions. The scatter plots (Fig. S3a-b) show the estimated TBG contributions to surface O₃ versus the model biases at surface sites. The correlation r values are weak for all points (i.e., -0.186 and -0.116 for MDA8 and W126, respectively). Our findings are qualitatively similar as those by Lin et al. (2012b).

We further separated the estimated TBG contributions by model biases at surface sites (Fig. S3c-d show the location of low and high bias sites), using the thresholds of ± 10 ppb and ± 5 ppm-h for MDA8 and W126, respectively, and plotted the histograms of the corresponding TBG contributions (Fig. S3e-h). For MDA8, the model-estimated TBG contributions that have high ($> \pm 10$ ppb) and low ($\leq \pm 10$ ppb) biases are both in the range of 26-42 ppb, with the medians of ~30-35 ppb. The Region 10 points (in green) have an additional 5-10 ppb of positive bias compared to the points with low biases, and the TBG contributions are ~35-42 ppb, indicating that the additional TBG led to the additional biases in total O₃. The TBG addition to total MDA8 over Region 10 is close to linear, due to relatively slow local O₃ photochemistry (more NO_x-limited regime, with more clouds and lower temperatures). The histogram of TBG contributions to W126 at sites with low model biases ($\leq \pm 5$ ppm-h) shows three peaks at ~3-4, ~10-12 and 15-17 ppm-h, while the plot of TBG contributions to W126 at sites with high model biases ($> \pm 5$ ppm-h) has a narrower span, and the first peak (Region 10 points in green) shift to ~5-12 ppm-h. Again, the 5-10 ppm-h of shift indicates that the overestimation in TBG led to the higher biases in total O₃ over Region 10.

This discussion is based on the analysis of the biases only at surface sites that had >75% of the daytime observations during the study period. Therefore, it depends on the spatial distributions of these sites, most of which are located in CA.

Table S1. Wildfire plumes characteristics from the Multi-angle Imaging SpectroRadiometer (MISR) plume height project ^a

| Region | Year | Number of plumes w/ power estimates | Total radiative of power (MW) | Median value of plume top heights (m ASL) | Radiative power/plume (MW) |
|------------------------------------|------|-------------------------------------|-------------------------------|---|----------------------------|
| Siberia | 2002 | 541 | 269422 | 1367 | 498.01 |
| | 2003 | 985 | 474288 | 2225 | 481.51 |
| | 2006 | 433 | 148157 | 1597 | 342.16 |
| | 2008 | 1451 | 574766 | 1652 | 396.12 |
| Canada (end of May to end of July) | 2008 | 72 | 92439 | 2062 | 1283.9 |
| North America | 2002 | 445 | 371717 | 1815 | 835.32 |
| | 2004 | 1137 | 501585 | 1743 | 441.15 |
| | 2005 | 912 | 376329 | 1415 | 412.64 |
| | 2006 | 439 | 253488 | 2191 | 577.42 |
| | 2007 | 510 | 237497 | 1620 | 465.68 |

^a Adapted from: <http://misr.jpl.nasa.gov/getData/accessData/MisrMinxPlumes/>

Table S2. US Geological Survey (USGS) land type numbers and descriptions ^a

| Land type number | Land type description | Category used in Figure 3 |
|------------------|--|---------------------------|
| 1 | Urban and Built-up Land | / |
| 2 | Dryland Cropland and Pasture | |
| 3 | Irrigated Cropland and Pasture | |
| 4 | Mixed Dryland/Irrigated Cropland and Pasture | Cropland |
| 5 | Cropland/Grassland Mosaic | |
| 6 | Cropland/Woodland Mosaic | |
| 7 | Grassland | |
| 8 | Shrubland | |
| 9 | Mixed Shrubland/Grassland | Grass + Shrub |
| 10 | Savanna | |
| 11 | Deciduous Broadleaf Forest | |
| 12 | Deciduous Needleleaf Forest | |
| 13 | Evergreen Broadleaf | Forest |
| 14 | Evergreen Needleleaf | |
| 15 | Mixed Forest | |
| 16 | Water Bodies | / |
| 17 | Herbaceous Wetland | / |
| 18 | Wooden Wetland | / |
| 19 | Barren or Sparsely Vegetated | / |
| 20 | Herbaceous Tundra | / |
| 21 | Wooded Tundra | / |
| 22 | Mixed Tundra | / |
| 23 | Bare Ground Tundra | / |
| 24 | Snow or Ice | / |

^a Adapted from: http://www.mmm.ucar.edu/wrf/users/docs/user_guide_V3/users_guide_chap3.htm#_Land_Use_and

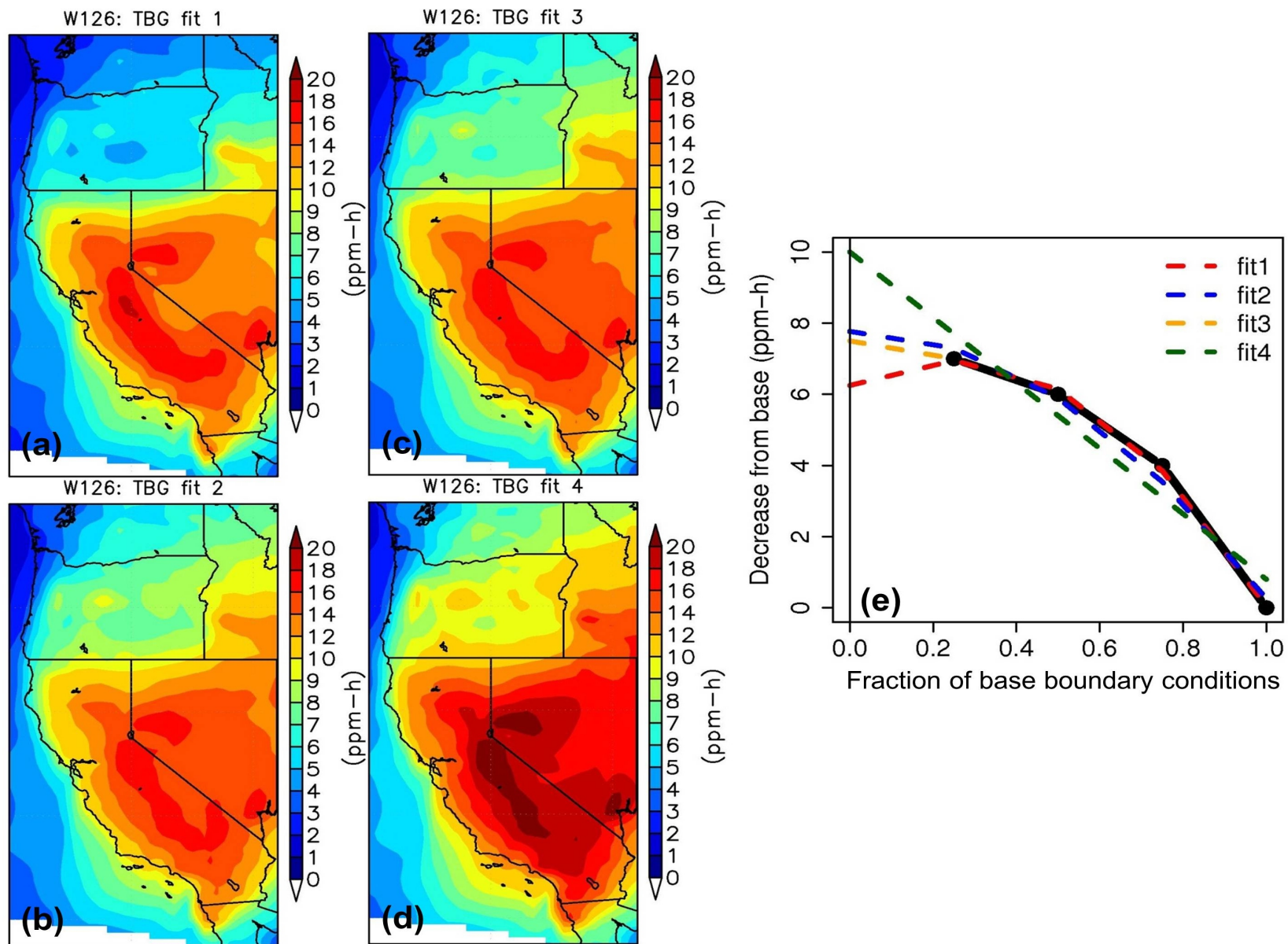


Figure S1. Spatial maps for estimated surface W126 contributed from TBG. The estimates in (a-d) were extrapolated by using four different methods described in Section S2 text. (e) Demonstration of extrapolation methods using the Regions 9 and 10 mean sensitivities to BC O₃ perturbations.

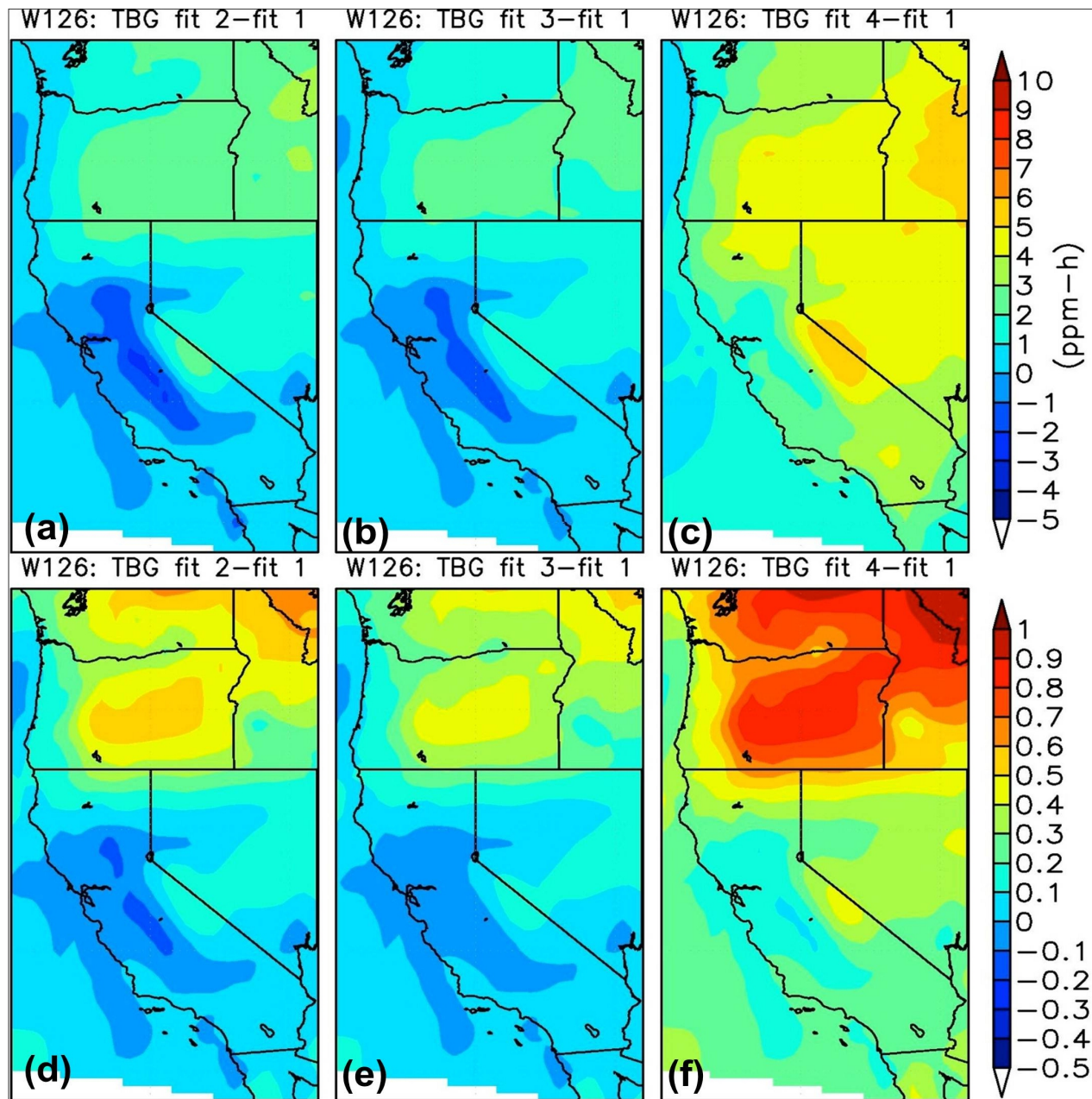


Figure S2. (a-c) Absolute and (d-f) relative differences between the extrapolated W126 contributed from TBG, calculated from values shown in Figure S1a-d.

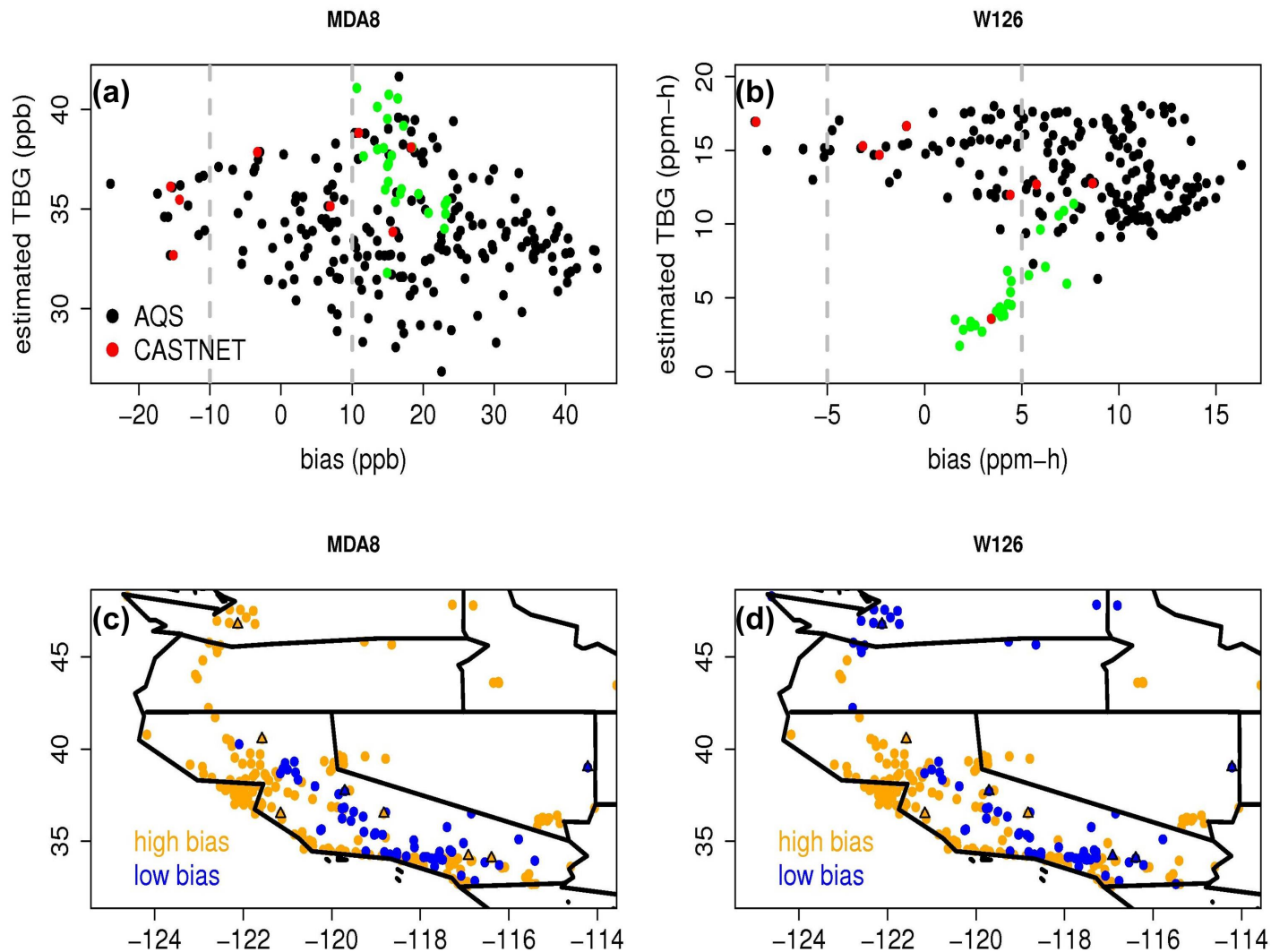


Figure S3. Scatter plots of the extrapolated TBG contributions (O_3 and several precursors) versus the model biases, based on the base results from the 60 km/18L model grid and AQS/CASTNET observations for (a) MDA8 and (b) W126. Black and red represent AQS and CASTNET sites, respectively. Green represents AQS sites over EPA Region 10 (states of Washington, Oregon and Idaho). Spatial distributions of the low/high-bias sites for (c) MDA8 and (d) W126. The thresholds for separating low and high biases regions are 10 ppb and 5 ppm-h for MDA8 and W126, respectively. Dots and triangles represent AQS and CASTNET sites, respectively.

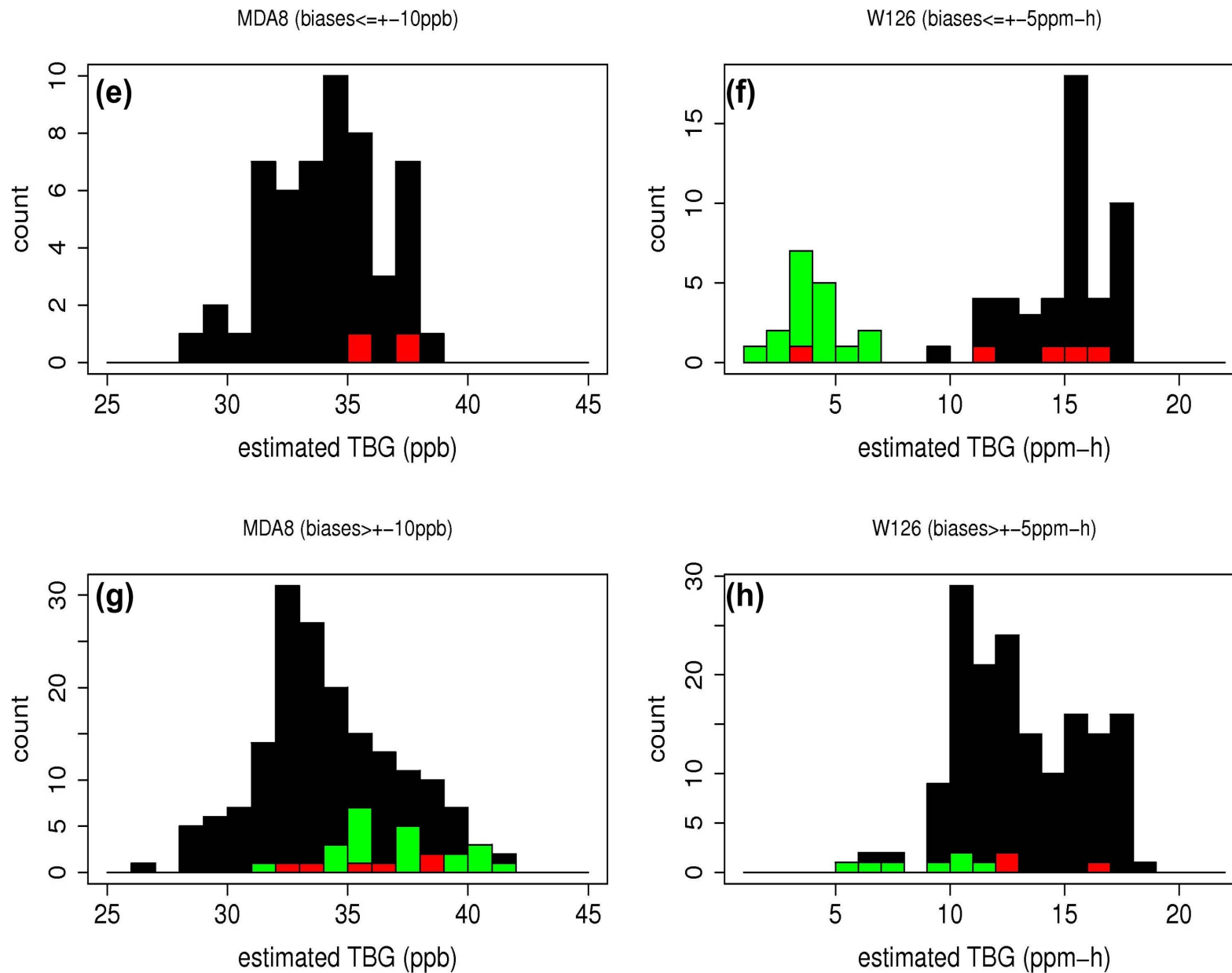


Figure S3 (cont.). Histograms of extrapolated TBG contributions over the (e-f) low biases regions and (g-h) high biases regions, for (e;g) MDA8 and (f;h) W126, respectively.

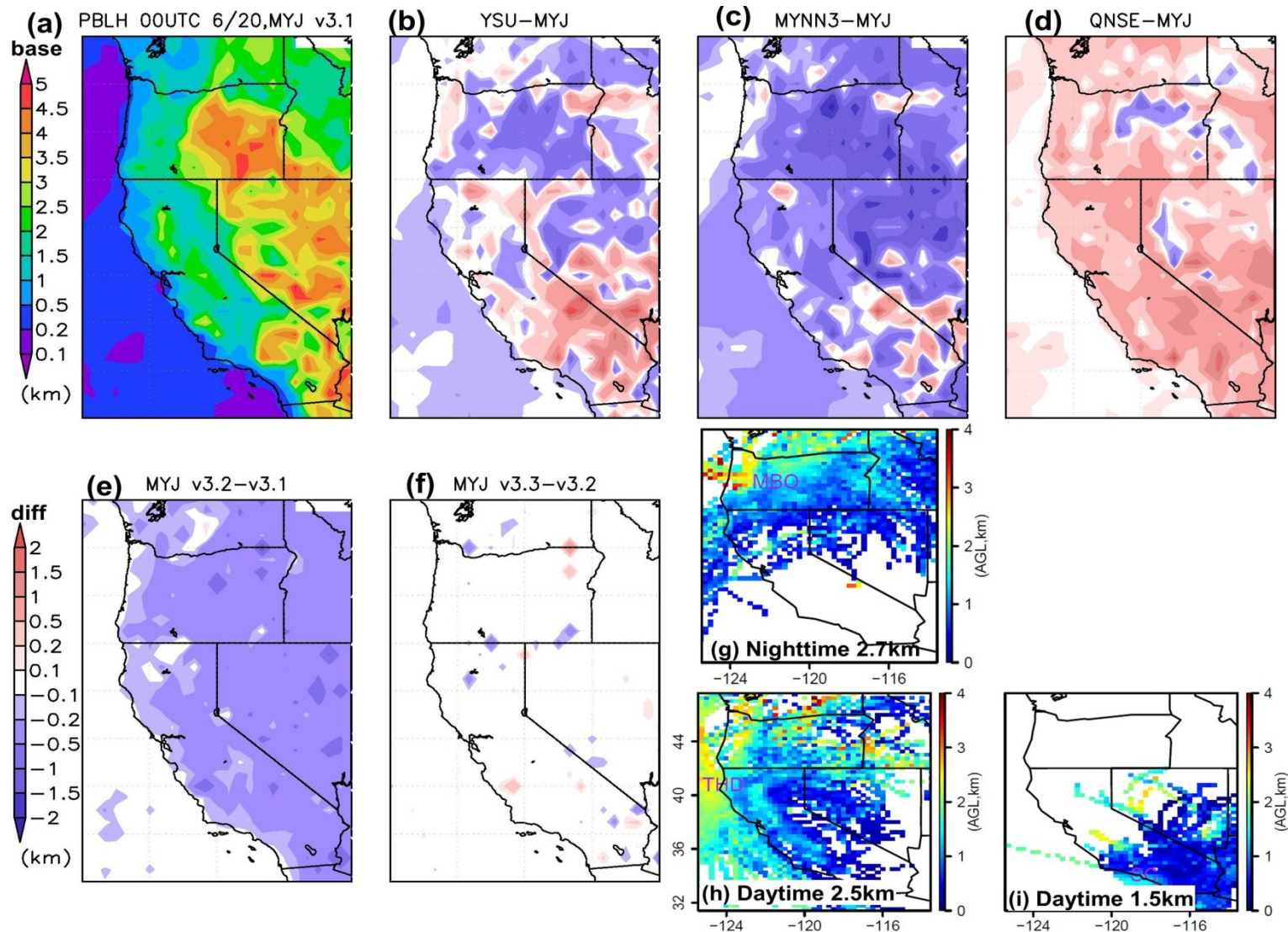


Figure S4. (a) 12 km WRF (Version 3.1)-predicted PBLH at 00 UTC, 20 June, by using the MYJ PBL scheme; Differences of WRF-predicted PBLH between the cases using (b) YSU; (c) MYNN3; and (d) QNSE PBL schemes and the results in (a); Differences of predicted PBLH between the cases using (e) WRF Version 3.2 and (f) WRF Version 3.3 and the results in (a); Similar as findings by Saide et al. (2011) over Santiago, Chile, overall MYNN3 and QNSE schemes generate the shallowest and deepest PBLH, respectively, and the differences between YSU and MYJ schemes vary by region. (g) PDT 9pm-7am forward trajectories (calculated mean transport altitudes in km, AGL for every 0.25 degree) during the study period originating from MBO 2.7 km ASL; PDT 8am-8pm forward trajectories during the studied period originating from (h) THD 2.5 km ASL and (i) SC 1.5 km ASL.

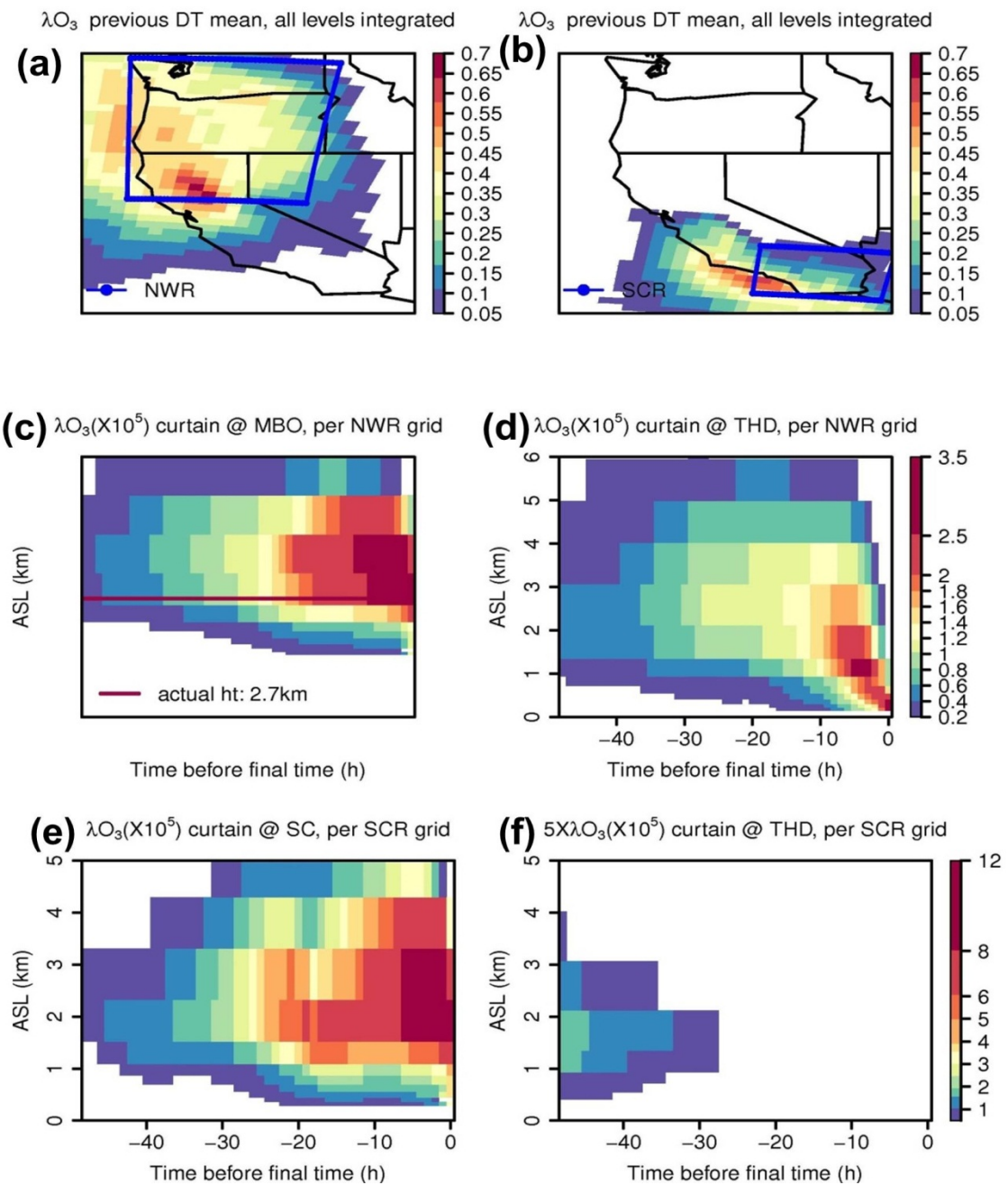
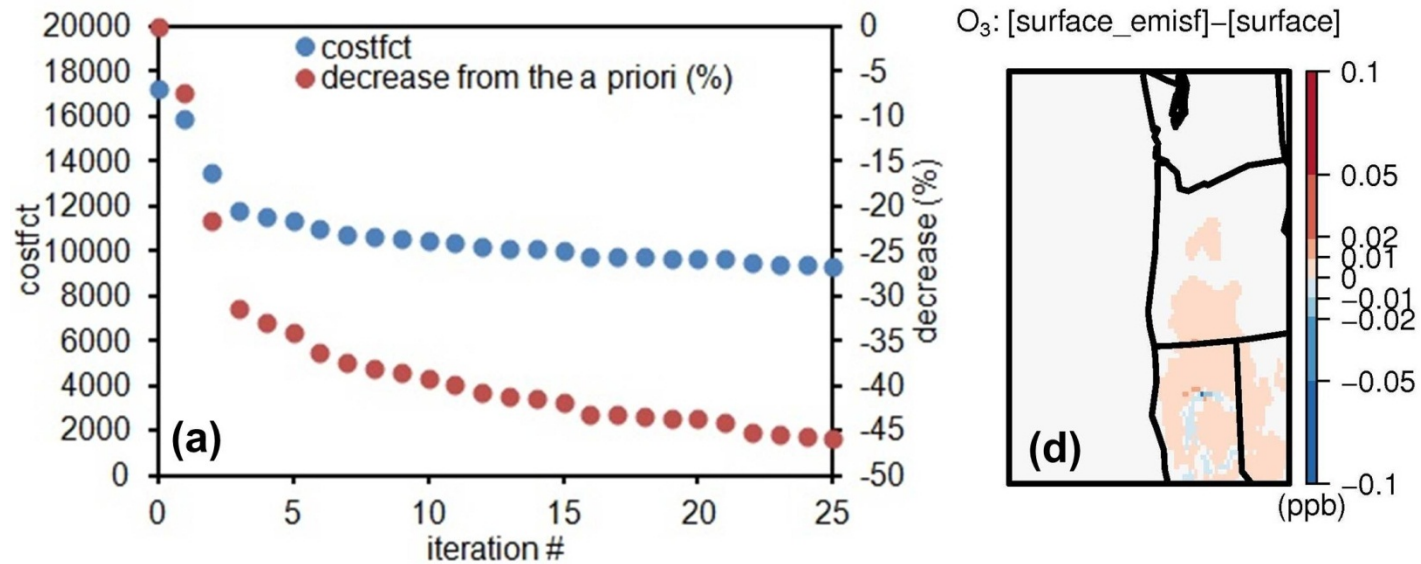
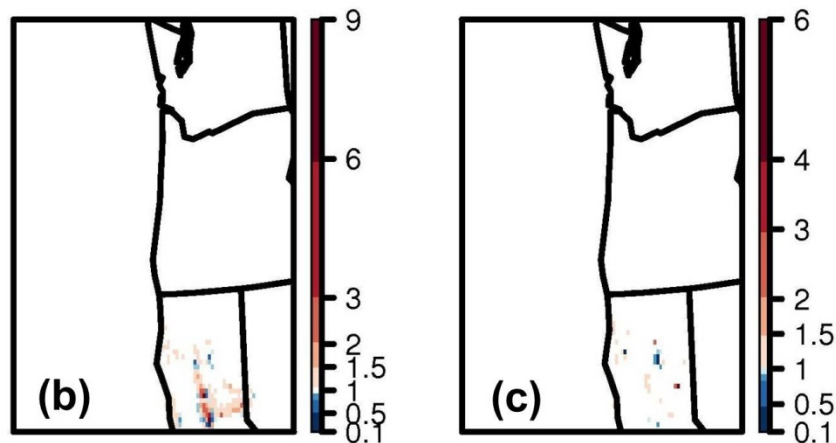


Figure S5. Same as Figure 9 but for results from the 60 km/18 layer grid.



Surface NO_x emission factors Elevated NO_x emission factors



Total emission adjustment: 1.002546

Figure S6. (a) Cost function and its reduction as a function of iteration number in Case AS; (b) Surface and (c) elevated NO_x emission scaling factors by controlling NO_x emissions and assimilating surface NO_2 observations in a 24-hour window; (d) Daytime mean surface O_3 differences: assimilating surface observation while applying NO_x emission scaling factors-Case AS.